

Article

Valorization of Dredged Sediments in Manufacturing Compressed Earth Blocks Stabilized by Alkali-Activated Fly Ash Binder

Mohamedou Brahim ^{1,*}, Khadim Ndiaye ¹, Salima Aggoun ¹ and Walid Maherzi ^{2,*}

¹ Laboratory of Mechanics and Materials of Civil Engineering (L2MGC), CY Cergy Paris University, 95000 Cergy Pontoise, France; khadim.ndiaye@cyu.fr (K.N.); salima.aggoun@cyu.fr (S.A.)

² Laboratory of Civil Engineering and Geo-Environment (LGCgE), Materials and Process Department, IMT Nord Europe, 59000 Lille, France

* Correspondence: mohamedou.brahim@cyu.fr (M.B.); walid.maherzi@imt-nord-europe.fr (W.M.)

Abstract: The valorization of dredged sediments is a promising solution to reduce the strain on natural resources, which is in line with sustainable development goals. This study aims to evaluate the potential valorization of dredged sediment in manufacturing compressed earth blocks (CEBs). The CEBs were stabilized by a combination of fly ash (FA) with sodium hydroxide (NaOH). The stabilization was achieved by partial substitution of sediment for fly ash with six different percentages 10, 20, 30, 40, and 50% by weight. The CEBs samples were characterized in terms of structural, microstructural, mechanical, and thermal properties. The results showed that increasing FA content significantly improves the mechanical strength of CEBs, dry compressive strength ranges from 2.47 MPa to 9 MPa, whereas wet compressive strength ranges from 0.95 MPa to 6.9 MPa. The mechanical performance is related to the amount of alkali-activated fly ash gels, which bind the sediment grains and makes the CEBs more compact and resistant. The optimal dosage of alkali-activated fly ash to replace the sediment was between 10 and 20%. In this substitution range, mechanical performance and physical properties improved significantly. In addition, the thermal properties varied slightly with alkali-activated FA content.

Keywords: dredged sediments; valorization; compressed earth blocks; alkali-activated fly ash



Citation: Brahim, M.; Ndiaye, K.; Aggoun, S.; Maherzi, W. Valorization of Dredged Sediments in Manufacturing Compressed Earth Blocks Stabilized by Alkali-Activated Fly Ash Binder. *Buildings* **2022**, *12*, 419. <https://doi.org/10.3390/buildings12040419>

Academic Editor: Lech Czarnecki

Received: 1 March 2022

Accepted: 25 March 2022

Published: 31 March 2022

Publisher's Note: MDPI stays neutral with regard to jurisdictional claims in published maps and institutional affiliations.



Copyright: © 2022 by the authors. Licensee MDPI, Basel, Switzerland. This article is an open access article distributed under the terms and conditions of the Creative Commons Attribution (CC BY) license (<https://creativecommons.org/licenses/by/4.0/>).

1. Introduction

Each year, an enormous amount of sediment is dredged to maintain sufficient depth for safe navigation in the ports and waterways. Annually, around 50 million m³ of sediments are dredged in France, whereas for the whole of Europe, this volume reaches a value of 300 million m³ [1,2]. These dredged sediments need to be adequately managed by sea dumping or landfilling in accordance with existing regulations. Nationally and internationally, legislation is gradually tightening the requirements for land disposal and dumping [3]. In terms of protecting natural resources and assuring the application of environmental laws, nowadays in many countries, several initiatives are emerging in the fields of eco-materials and civil engineering. Dredged sediments are becoming increasingly considered as a source of construction materials and a suitable solution for sustainable development [4]. Nonetheless, a limited quantity of dredged sediment is used and recycled [5–7]. These sediments have a diverse range of characteristics. The provenance of these sediments, as well as the period of dredging over the year, have a significant impact on their constitution. Mineral particles (carbonates, quartz, different silicates, iron and manganese oxyhydroxides, and sulfides) make up the majority of sediments, along with some organic substances and inorganic pollutants [8–10]. The beneficial uses of dredged sediments in construction materials have been discussed in many forums. Dredged sediments have been successfully valorized in the manufacturing of Portland cement [11–13], aggregates [14], as well as in bricks production [15–19], and roads [20].

In this context, the development of building materials based on sediments that respect the environment and especially the ones adapted to the type of construction is being encouraged. In this respect, the compressed earth brick stands as a serious candidate.

The compressed earth blocks are the modern version of adobe blocks obtained by the use of machines allowing the production of perfectly calibrated blocks [21]. However, the use of sediment as raw material in the manufacturing of compressed earth blocks requires the identification of certain characteristics that should conform to requirements regarding particle size, plasticity, presence of organic substances, as well as dry density [17,18]. The existing standards and recommendations [22,23], have suggested some recommendations to allow for an adequate selection of materials to be used in the CEBs. For this purpose, the maximum size of particles is better to be 10 mm (it is not prescribed as minimum size, but it is necessary to have the presence of a minimum of 5% of clay which can act as a natural binder) [24]. The proportion of the clay fraction must not exceed 15% of the total mass in order to avoid the risk of cracking related to the shrinkage which makes the blocks vulnerable [21,22]. Approximately 15 and 30 is the recommended plasticity index [18,24], the dry density has to be in the range of 1600 to 2200 kg/m³ [21,24]. Following standard NF XP P13-901, the compressive strength of CEBs should be superior to 2 MPa. According to many studies carried out on compressed earth blocks [25–27], their results indicate compressive strengths ranging between 1.4 to 20 MPa, and Young's modulus values scale of 1 to 11.5 GPa.

The earth materials are very sensitive to water and environmental changes due to high moisture absorption capacity that can contribute to their rapid degradation [28,29]. These disadvantages generated a great interest in the research of innovative solutions. More recently, chemical stabilization essentially consists of the technique of mixing additives with soil, has become a common approach to improve the mechanical strength and durability of CEBs. Indeed, the stabilizers most often used are cement and lime, but there are also other stabilizers of different origins (animal, vegetable, or industrial by-products) such as alkali-activated binders, palm fibers, and bitumen. Alkali-activated binders appear as alternative binders. They could replace Portland cement in the manufacture of compressed earth blocks. Moreover, these products are energy efficient since they reduce carbon emissions compared to Portland cement [28]. An alkali-activated binder is obtained by the polycondensation of aluminates and silicates with alkaline activators giving polymeric Si-O-Al bonds [30]. Recent research [19], has shown that the use of dredged sediment as a raw material of compressed earth blocks combined with 5% glass and 10% blast furnace slag satisfies the strength and water resistance criterion suggested by different standards. Sore et al. [27] carried out a series of experiments on lateritic CEBs stabilized by an alkali-activated binder (metakaolin(MK) with sodium hydroxide). The results showed that the addition of MK \geq 20% satisfy the required characteristic strength of 4 MPa, and the total water absorption and durability were improved significantly. Very interesting results have been obtained by using alkali-activated binders as earth blocks stabilizer.

The primary objective of this research is to evaluate the feasibility of employing dredged sediments as raw materials to produce CEBs. An experimental program was developed to identify the appropriate mixing ratios for the laboratory production of compressed earth blocks using dredged sediments as the main constituent, alkali-activated binder based on fly ash, and sodium hydroxide solution as a stabilizer. Physical and chemical characteristics of all raw materials (dredged sediments, fly ash) were examined initially. Then, the CEBs samples were prepared by varying the dredged sediments and fly ash content. Subsequently, the physical, mechanical, and thermal properties of the prepared blocks were studied. The leaching test results are not included in this paper, however, the Findings validated that the sediment can be classed as non-hazardous waste, based on the leaching limits for inert waste prescribed in (French Directive 0289 published on 14 December 2014) [31].

2. Materials and Methods

2.1. Materials

2.1.1. Dredged Sediments

The dredged sediments have been taken from the north of France at the European Metropolis of Lille (MEL) and used in the experimental program. According to the standard's recommendations, these sediments were sieved and classed as granular particles with a diameter of 0–5 mm [22]. The Figure 1 shows the particle size distribution of the sediment and the standard range according to NF XP P13-901 [22]. It should be noted that part of the sediment curve is outside the recommended range. However, it is generally accepted that many soils that fall outside the recommended range can, in practice, give acceptable results [22]. Using the soil's classification nature [22], the sediments were classified as type B2 (B2 acceptable material with a little insufficiency of fines) based on physical properties including particle size distribution, plasticity index (14.4%), and methylene blue value (1.3).

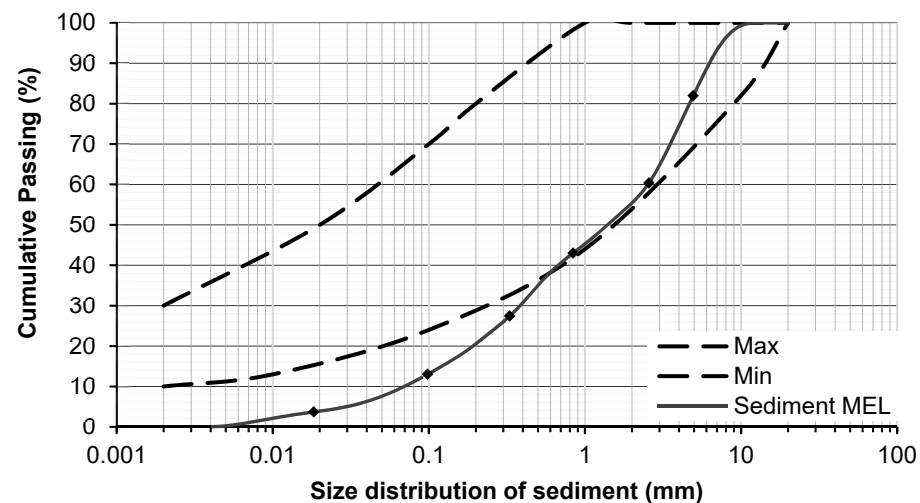


Figure 1. Particle size distribution of sediment Min, Max standard NF XP P13-901 [22].

The physical properties of dredged sediments are presented in Table 1.

Table 1. Physical properties of sediment.

Characterization	Sediment	Standard Used
Clay (<2 μm)	1.80	NF ISO 13320-1
Silt (2–63 μm)	30.57	
Sand (>63 μm)	67.41	
Liquid limit Wl (%)	63.54	NF P94-051
Plastic limit Wp (%)	49.13	
Plasticity index Ip (%)	14.41	
Methylene blue value (VBS)	1.3 g/100 g	NF P94-068
Density Gs (g/cm^3)	2.39	NF EN 1097-7
LOI (450 $^{\circ}\text{C}$) (%)	13.82	XP P94-047
Water content (%)	22.34	NF P94-050

The mineral composition was determined by X-ray diffraction (XRD) analysis. The Figure 2 shows XRD diffractogram of the sediment and indicated that Quartz (Q) and Calcite (C) predominate in the sediment, with less content of other mineral phases such as Kaolinite (K) and Chlorite (C_H). Chemical compositions of the dredged sediments were investigated using X-ray fluorescence (XRF) analysis.

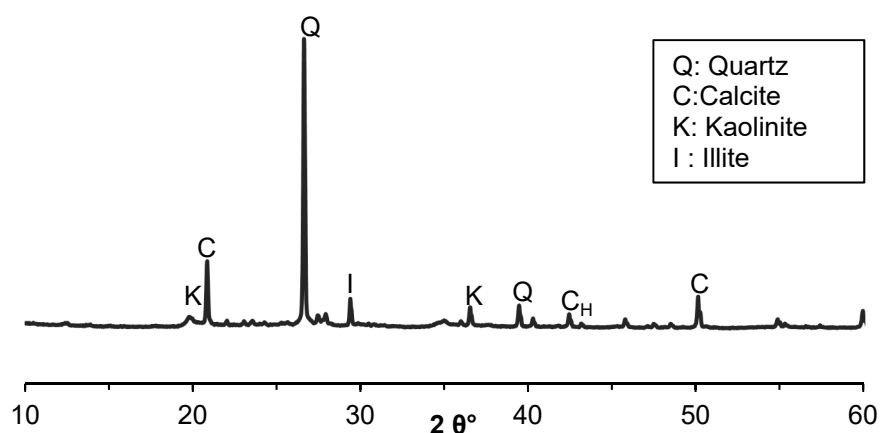


Figure 2. XRD mineralogical analysis of sediment.

The chemical composition of the sediment presented in Table 2 has revealed that the main oxide in the sediments is SiO_2 , together with Al_2O_3 , CaO , and Fe_2O_3 .

Table 2. Chemical composition of sediment.

Oxide Content (%)	Sediment
SiO_2	51.9
Al_2O_3	11.1
CaO	13.3
Fe_2O_3	4.7
Na_2O	0.6
K_2O	3.8
MgO	1.6
TiO_2	0.5

2.1.2. Class F Fly Ash

The fly ash (FA) used in this study was supplied by the company SURSCHISTE (Lens, France). It was obtained from coal-fired power plants and has an absolute density of 2.39 g/cm^3 and a Blaine fineness between 2300 and 5000 g/cm^2 . According to EN 450-1 [32], the fly ash used is class F. The FA consists mainly of SiO_2 (50%), Al_2O_3 (20%) and Fe_2O_3 (8%). It is composed of minerals phases such as quartz (SiO_2), maghemite ($\gamma\text{-Fe}_2\text{O}_3$), mullite ($\text{Al}_6\text{O}_{13}\text{Si}_2$) and hematite ($\alpha\text{-Fe}_2\text{O}_3$). The properties of fly ash are shown in Table 3.

Table 3. Properties of fly ash.

Characterization	Fly Ash
Specific Gravity g/cm^2	2300–5000
Major minerals	Quartz (SiO_2)
	Maghemite ($\gamma\text{-Fe}_2\text{O}_3$)
	Mullite ($\text{Al}_6\text{O}_{13}\text{Si}_2$)
SiO_2 (50%) + Al_2O_3 (20%) + Fe_2O_3 (8%)	78%

2.1.3. Sodium Hydroxide Solution

To activate the fly ash, industrial-grade (NaOH) with a purity of 99% was utilized. The sodium hydroxide solution concentration was fixed to 8 M for all mix-designs. This concentration is the optimal activator content generating fly ash reaction according to the literature [33]. The activation solution was prepared and cooled at 20°C for 24 h before performing the mix-design.

2.2. Methods

2.2.1. Optimal Water Content

The optimum soil water content is the water amount that produces the highest dry density for a given energy of compaction. If the water content of the soil is too high, the compaction pressure will be dispersed by the water trapped between the particles [34]. Whereas the particles will not be adequately lubricated if the water content is low and compacting the soil to its minimal volume would be unattainable. The standard Proctor compaction test was used to determine the optimal water content of the different dry mixtures presented in Figure 3. Due to its fine grain size, the increase of fly ash content generated higher optimal water content and a slight decrease in density [35].

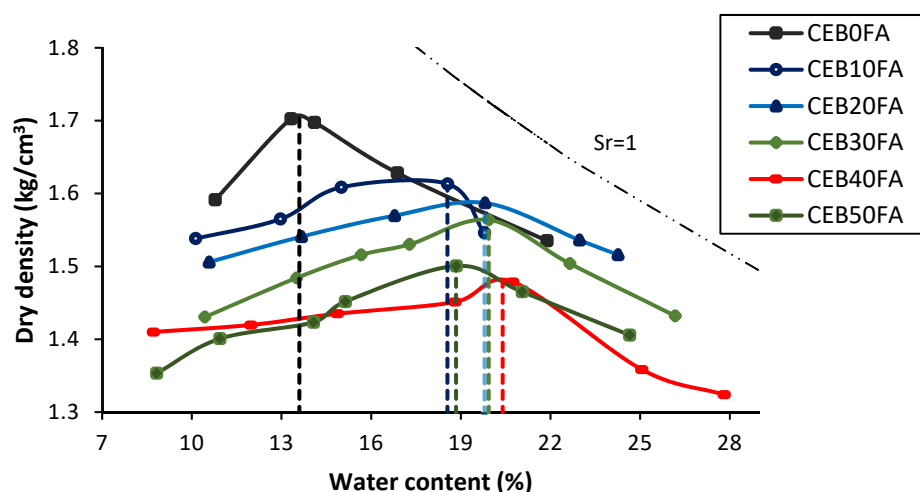


Figure 3. Optimum water content of dry mixtures.

2.2.2. Preparation of CEBs

The preparation of the mixture to produce a compressed cylindrical specimen of dimension 50 mm diameter and 100 mm height was carried out in two stages. After homogenizing the dry mixture (sediment and fly ash) for 7 min, wet mixing followed by adding the prepared alkaline activation solution with the corresponding water content to the optimum Proctor and the sodium hydroxide. The resulting mixtures were compacted using an INSTRON machine model (INSTRON-3369) with static compaction at a pressure of 40 bars. The cylindrical metallic molds were equipped with three wedges of different heights. Static compression was performed in three states with a system of smaller and smaller compression metallic wedges used at each phase. This method makes it possible to progressively obtain the final dimension of the sample according to the standard NF P 94-100 [34]. After compressing the sample, the load was kept for 10 s, and then the specimens were removed from molds using a demolding piston (as seen in Figure 4).

Following the manufacturing phase, the stabilized blocks were packed in plastic bags and placed in an oven at 50 °C for seven days, then the samples were placed in with ambient temperature until the 28th day for curing to minimize the problem of efflorescence (as suggested in the literature) [36]. After their specific cures, the blocks were characterized physically, mechanically, and thermally.

The details of the compositions of the mixture including raw materials (sediment, fly ash), water content and NaOH solution, used in the manufacturing of the CEBs are given in Table 4.

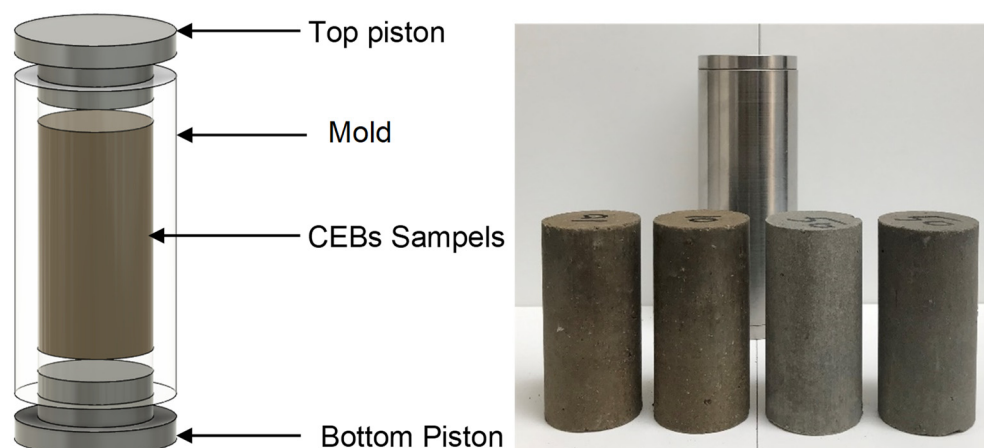


Figure 4. Preparation of CEBs samples.

Table 4. Composition of CEBs mix-designs.

Materials	CEB0FA	CEB10FA	CEB20FA	CEB30FA	CEB40FA	CEB50FA
Sediment (%)	100	90	80	70	60	50
Fly ash (%)	0	10	20	30	40	50
Water */dry material (%)	0.1409	0.1855	0.2187	0.1993	0.207	0.1884
NaOH concentration (Mol/L)	8	8	8	8	8	8

* Water content (%).

2.2.3. Experimental Techniques

The granulometry analysis was carried out using a COULTER LS12330, a laser device for detecting the dispersion of granular particles with a diameter of less than 0.1 μm (NF ISO 13320-1). The mineralogical composition was determined by X-ray diffraction BRUCKER AXS D8 ADVANCE using the $\text{CuK}\alpha$ radiation ($=1.78 \text{ \AA}$). The settings are 40 kV and 40 mA voltage. A BRUCKER S4 for X-ray fluorescence spectrometry measurements was used to identify the chemical composition. A scanning electron microscope Gemini 300 (ZEISS) scanning electron microscope Gemini 300 (ZEISS) coupled with a Quantax 10 (Bruker) X-ray microanalysis detector was used to analyze the microstructure with a focal distance of only 8.8 mm and acceleration voltages of 10 kV. An alpha spectrometer with an attenuated total reflection cell (ATR) was used to record FTIR spectra on crushed samples. Transmission spectra between 4000 and 400 cm^{-1} were collected.

Physical parameters of CEBs, including bulk density and porosity, were calculated using Equations (1) and (2) of EN NF 1936 standard [37]. To avoid the probable dissolution of CEBs, absolute ethanol was used as an alternative to water.

$$\rho = m_{dry} \times \rho_{eth} \left(\frac{M_{sat.air} - M_{sec}}{M_{sat.air} - M_{sat.eth}} \right) \quad (1)$$

$$\varepsilon = 100 \times \left(\frac{M_{sat.air} - M_{sec}}{M_{sat.air} - M_{sat.eth}} \right) \quad (2)$$

where ρ , bulk density; ρ_{eth} , density of ethanol; M_{dry} , dry mass (g); $M_{sat.air}$, saturated mass in air (g); $M_{sat.eth}$, saturated mass in (g); and ε , accessible porosity (%).

The dry and wet compressive strengths were carried out according to XP P13-901 [22], using a 0.15 kN/s loading rate three samples were examined for each test, and the results presented are the average of the tested specimens. The tests were carried out using a hydraulic press with a maximum load capacity of 30 kN. The wet compressive was performed on CEBs that had been immersed in water for 2 h. The dynamic modulus of elasticity was measured by the ultrasonic velocity method which consists in the transmission of an ultrasonic wave in the samples.

The hot disc method was used to determine the thermal characteristics under controlled room temperature (20 °C and 50% RH).

The water Absorption by Capillarity of CEBs was measured in accordance with XP P 13-901 Standard [22]. The dry blocks were first weighed, then placed in a thin layer of water (5 mm) for 10 min for the water absorption test.

3. Results

3.1. Microstructural Properties

The microstructure of the blocks (CEB0FA, CEB10FA, CEB40FA, and CEB50FA) are shown in Figure 5. The unstabilized blocks Figure 5a tend to have a very porous structure with apparent sand and silt particles. Cracks are also observed, which are due to desiccation shrinkage according to Jaditager et al. [38]. Figure 5b–d reveals the microstructure of stabilized blocks which shows densification by physical (compaction) and chemical (geopolymerization) effects. Indeed, as the addition of fly ash increases, the cohesion between the sediment grains becomes stronger. Figure 5c,d indicates that the CEB40FA and CEB50FA have a more compact matrix with partially dissolved fly ash particles. Densification of the matrix is observed with increasing alkali-activated fly ash content. This is consistent with the experimental results reported in (Section 3.2), showing lower porosity for CEB50FA.

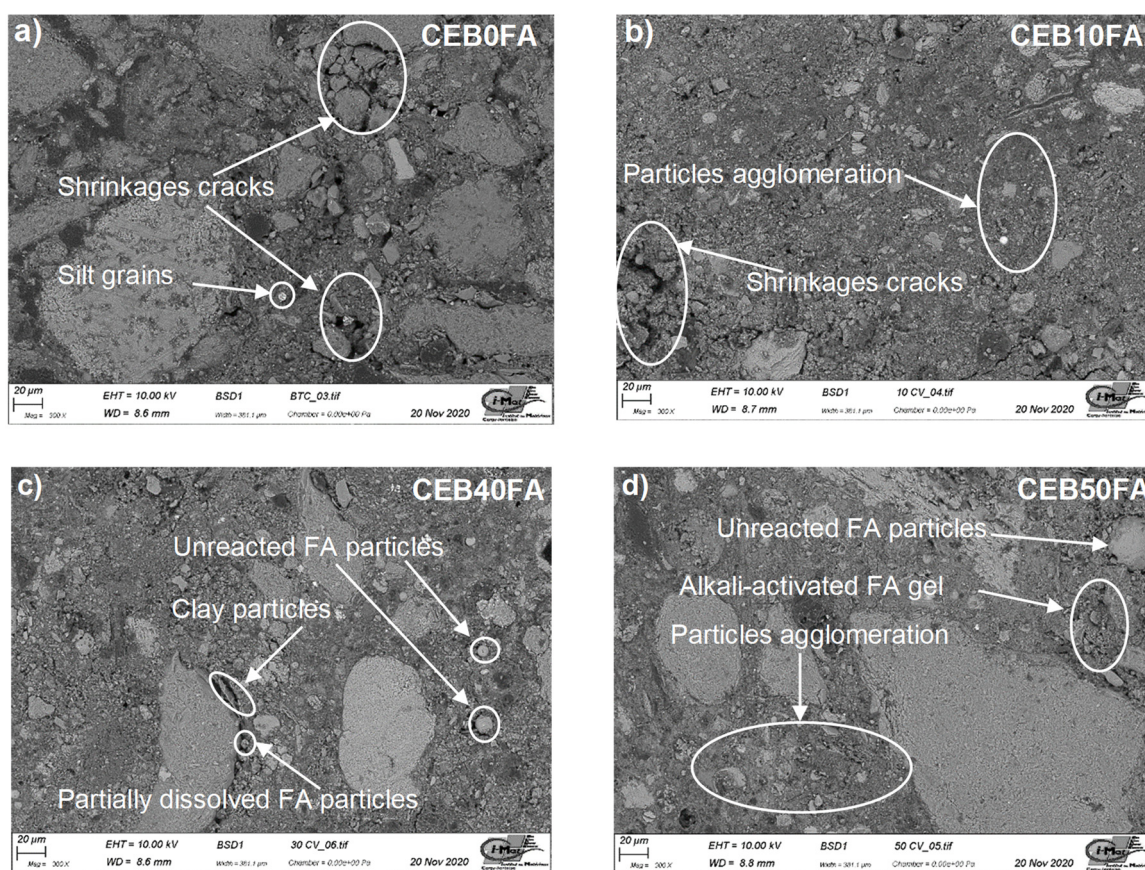


Figure 5. SEM images of CEBs: (a) CEB0FA; (b) CEB10FA; (c) CEB40FA; and (d) CEB50FA.

A complete dissolution of fly ash in an alkaline solution (NaOH) is not achievable, hence the unreacted or partially dissolved fly ash particles noted on stabilized CEBs [38]. According to Adam et al. [39], unreacted and partially dissolved fly ash particles form a non-negligible fraction of the overall volume of the alkali-activated binder and are predicted to improve mechanical strength. They act as binding elements in the sediment-fly ash matrix. Therefore, these variations in the microstructure have a substantial influence on the

physical, mechanical behavior, and durability of the blocks. The observed microstructural changes of the stabilized blocks are attributed to the formation of the alkali-activated gels which strengthens the bonds between the sediment particles.

The different blocks were subjected to Fourier transform infrared spectroscopy (FTIR) analysis to identify the chemical events that appear with stabilization the spectral curves are displayed in Figure 6. Samples of unstabilized blocks (CEB0FA) showed peak around the 975 cm^{-1} wavenumber linked to an Al-O bond which translates the presence of alumina and the 1400 cm^{-1} peak is associated with a C-O bond [40]. In addition, a water absorption band was recorded at 1630 cm^{-1} and 3350 cm^{-1} for CEB0FA [7].

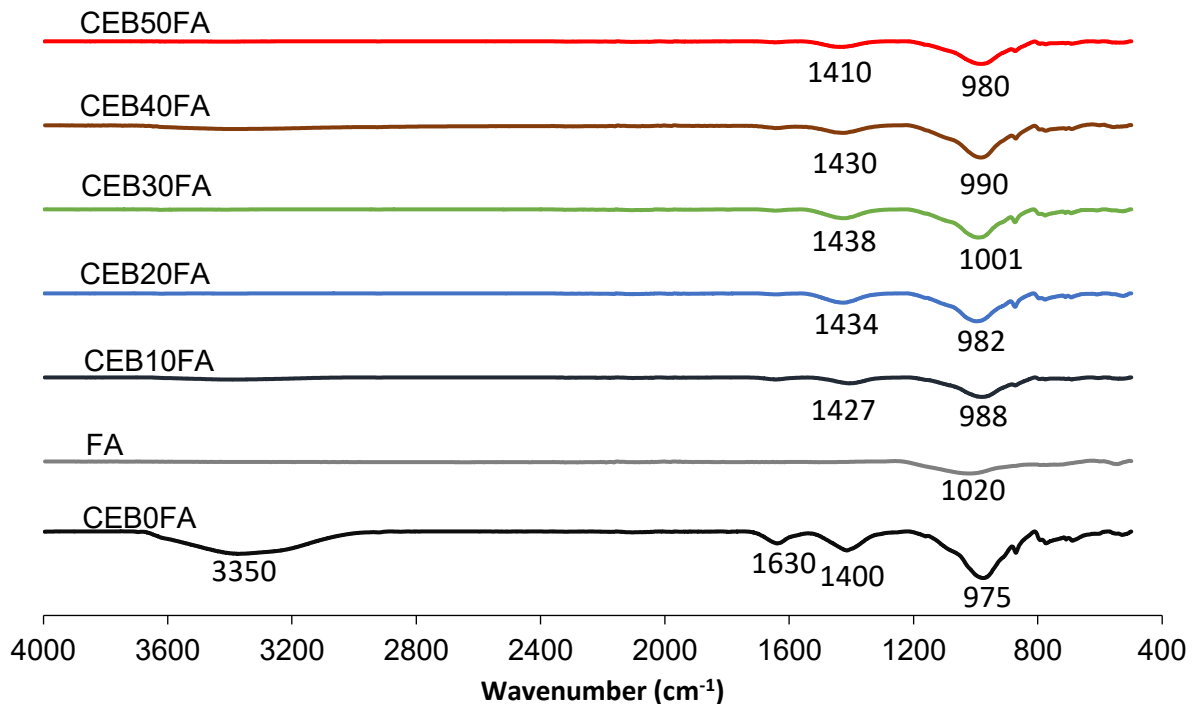


Figure 6. FTIR spectra of fly ash and different CEBs.

The peak for FA has shifted from 1020 cm^{-1} for unreacted fly ash to 980 cm^{-1} for CEB50FA. This absorption band shift is related to the fly ash particle's reaction. Furthermore this displacement of the band corresponding to the elongation vibrations of the Si-O-Si or Si-O-Al groups to lower wavenumber is due to the fly ash reaction and the formation of a new products [33,41].

3.2. Physical Properties

Porosity is one of the influential factors that affect the mechanical properties of compressed earth blocks [27]. Figure 7 shows the results of porosity and bulk density of the synthesized CEBs. The porosity was directly related to the fly ash content. It decreases linearly with the increase in fly ash content. This could be explained by the fact that the hydration of the fly ash caused the precipitation of hydrates filling the porosity. On the other hand, the presence of fine particles of fly ash was included in the sediment skeleton, thus making it possible to fill the voids between the other larger sediment particles (improvement of the granular compactness). Furthermore, the density of the blocks varies between 1600 and 1850 kg/m^3 and is linearly related to the fly ash content [42].

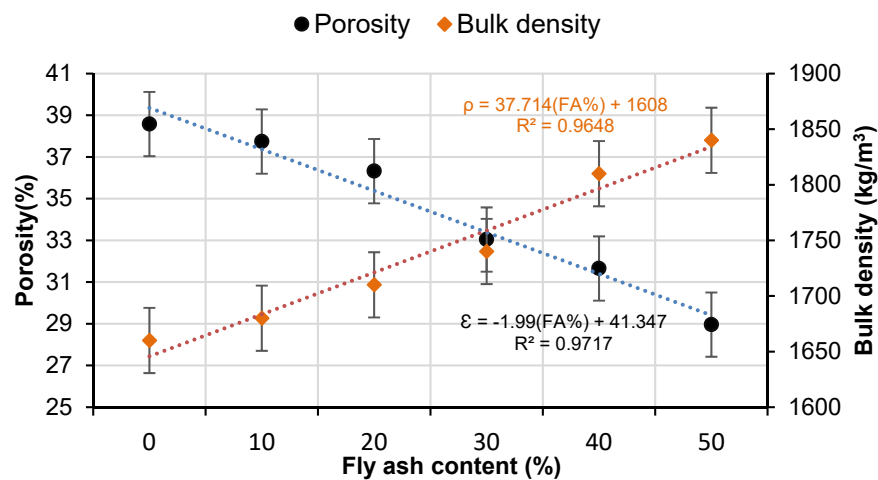


Figure 7. Porosity and bulk density of CEBs as a function of fly ash content.

3.3. Mechanical Properties

The dry compressive strength of unstabilized CEBs changes from 2.4 MPa for CEB0FA to 11.6 MPa for CEB50FA as shown in Figure 8. The mechanical strength increases with the fly ash content. The improvement in mechanical performance is related to the formation of hydrates which bind the sediment particles together and make the blocks more compact and resistant. After reaction with a sodium hydroxide solution, the fly ash dissolves and generates a very large number of $[\text{SiO}(\text{OH})_3]^-$ and $[\text{Al}(\text{OH})_4]^-$ combinations [27,33,43] that create alkali-activated gels. Due to the high concentration of the alkaline solution, the gels produced consist of a large three-dimensional aluminosilicate network that binds the sediment particles. The best mechanical strengths were obtained with the highest fly ash contents (CEB40FA, CEB50FA). Indeed, all CEBs stabilized with at least 10% fly ash have a compressive strength higher than 4 MPa recommended by the XP13-901 standard [22] for earthen constructions.

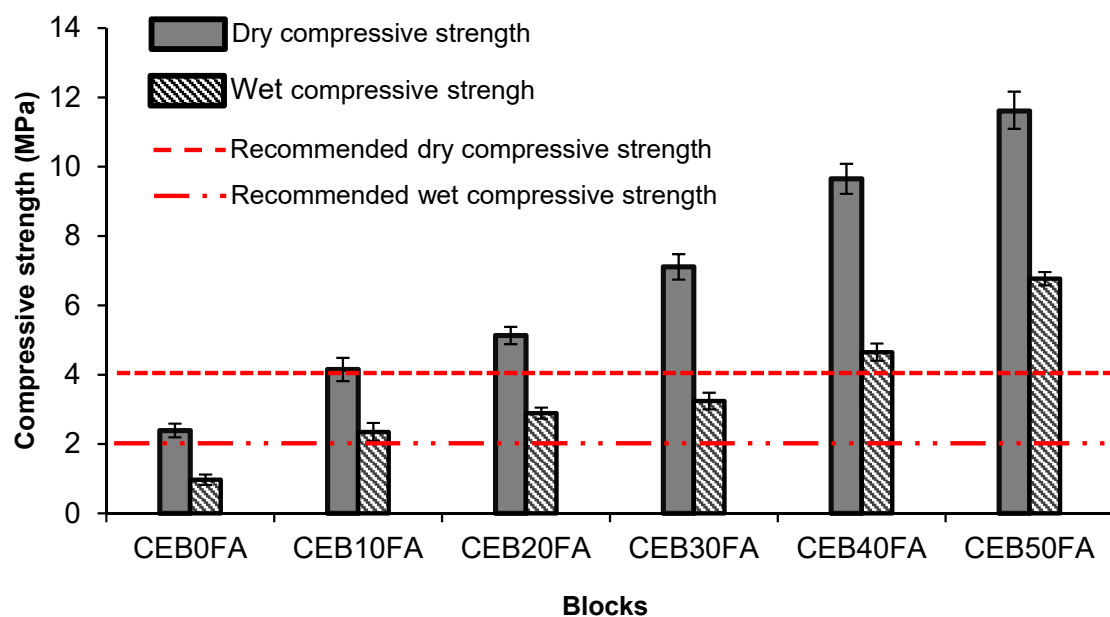


Figure 8. Dry and wet compressive strength of CEBs after 28 days.

The standards [21,22,41] classifies compressed earth blocks into two categories: blocks with compressive strengths ranging from 2 to 4 MPa used for non-bearing walls, and those with compressive strengths more than 4 MPa used for bearing walls [41]. Based

on the dry and wet compressive strengths, stabilized CEBs with at least 20% fly ash are suitable for bearing wall construction, and stabilized CEBs with 10% fly ash are applicable for non-bearing wall construction. The dynamic modulus of elasticity was measured in complement to the compressive strength. The obtained results vary between 2.07 and 8.7 GPa, and the values remain within the range found in the literature for other types of compressed earth blocks [27,44]. In the Figure 9, the dynamic modulus of elasticity increased linearly with the fly ash content. This linear relationship have been observed by Sore et al. [27], Islam et al. [44].

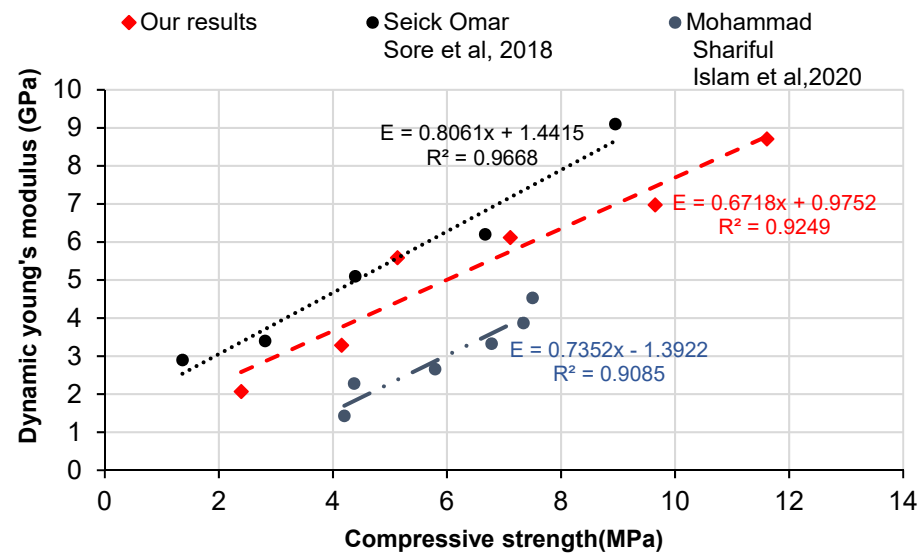


Figure 9. Correlation between Young's modulus and dry compressive strength.

3.4. Thermal Properties

In addition to mechanical strength, the thermal performance of compressed earth blocks is also important for maintaining thermal comfort inside buildings. Indeed, this thermal insulation capacity depends on certain parameters [41] including the nature of the material components [45], the water content [46], and the porosity [47]. Furthermore, bulk density is among the factors influencing brick thermal conductivity [48]. The variation in specific heat and thermal conductivity observed in Figure 10 could be related to a variation in the porosity of the materials, the intrinsic composition of each sample, and the cohesion of the material. Thus, the hydration of fly ash allows the formation of alkali-activated gels which ensures reinforcement of the bonds between the constituents of the sediment (sand, silt, and clay) and consequently favors a decrease in porosity which results in the creation of a continuous and homogeneous internal structure [49]. Hence, the heat transfer will be improved by this dense morphology. Concerning the specific heat, the highest value is obtained by CEB40FA (1130 J/kg·K) while the CEB0FA has the lowest value (1010 J/kg·K).

It should be noted that there is a slight increase in thermal conductivity with the FA content. The thermal conductivity remain of stabilized blocks remains close to that of unstabilized blocks. Indeed, the increase in the density of CEBs (decrease in porosity) led to thermal conductivity. Moreover, the correlation shown in Figure 11 is consistent with other studies which indicate a strong relationship between the thermal behavior of blocks and their density [42,47,48].

The Figure 12 exhibited a significant relationship between the thermal behavior of blocks and their bulk densities, which is consistent with previous studies [42,47,48]. This finding is consistent with the values found on laterite blocks stabilized by waste glass with a content ranging from 0 to 15% [48]. as well as by cement with a grade varying from 3 to 9% [42]. Furthermore, in RE2000 [50], a single value of 1.1 (W/m·K) is given for earth materials (rammed earth, compressed earth blocks), which is higher than all of our results. Therefore, earth buildings constructed by sediment CEBs would have the required

thermal isolation to create a suitable interior thermal comfort. Furthermore, these blocks are suitable for the building thermal performance (low-energy buildings with an energy consumption below 50 kWh/m²/year) imposed by RT2012 [51].

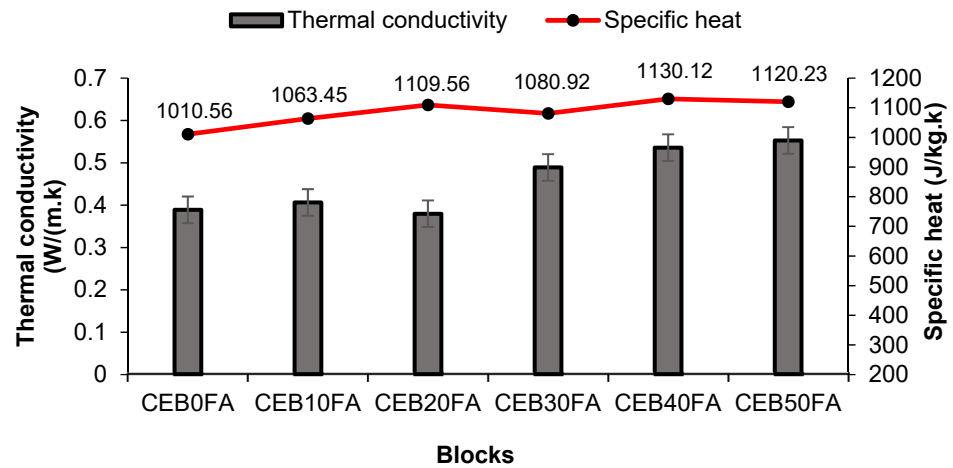


Figure 10. Thermal conductivity and specific heat of different CEBs.

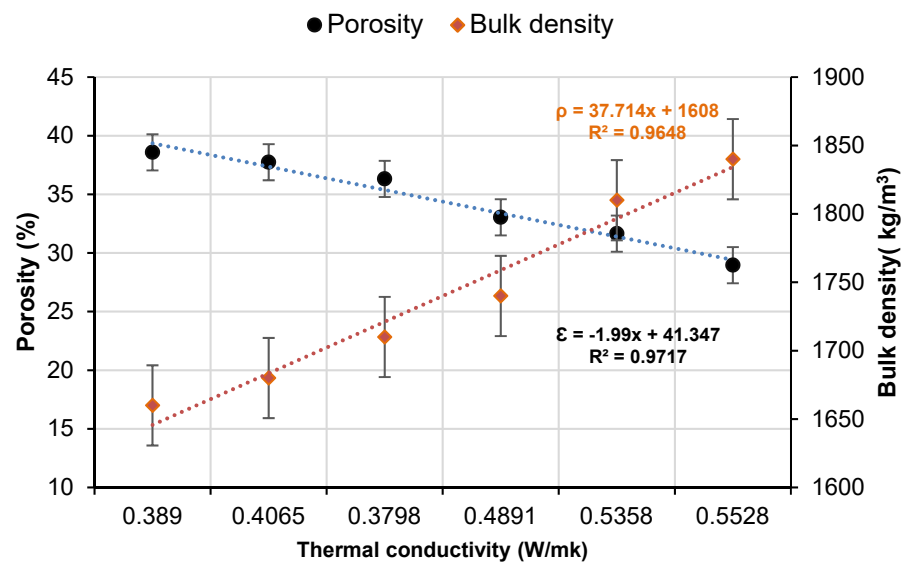


Figure 11. Relationship between thermal conductivity, porosity, and bulk density of CEBs.

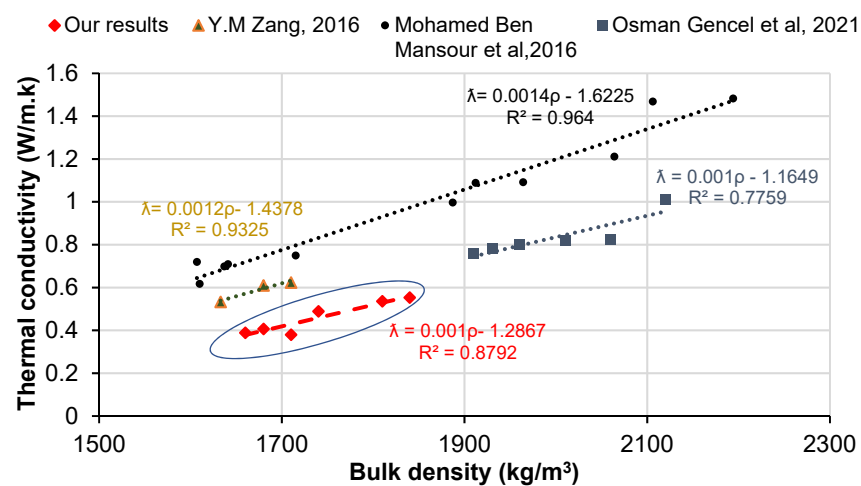


Figure 12. Relationship between thermal conductivity and brick density.

3.5. Water Capillary Absorption

The results of the water absorption by capillary test presented in the Figure 13 show a coefficient ranging from 18.08 and 8.23 $\text{g}/\text{cm}^2 \text{min}^{1/2}$ for stabilized blocks. Whereas for the unstabilized blocks, the coefficient obtained is 21.46 $\text{g}/\text{cm}^2 \text{min}^{1/2}$. The coefficient decreases with increasing alkali-activated binder content [52], which justifies the gap of 13% between CEB0FA and CEB50FA. All the stabilized blocks can be classified as low capillary blocks ($C_b < 20$), according to XP P13 901 [22]. Therefore, the stabilized CEBs prepared in this study meet the requirements for the application in the construction of external walls.

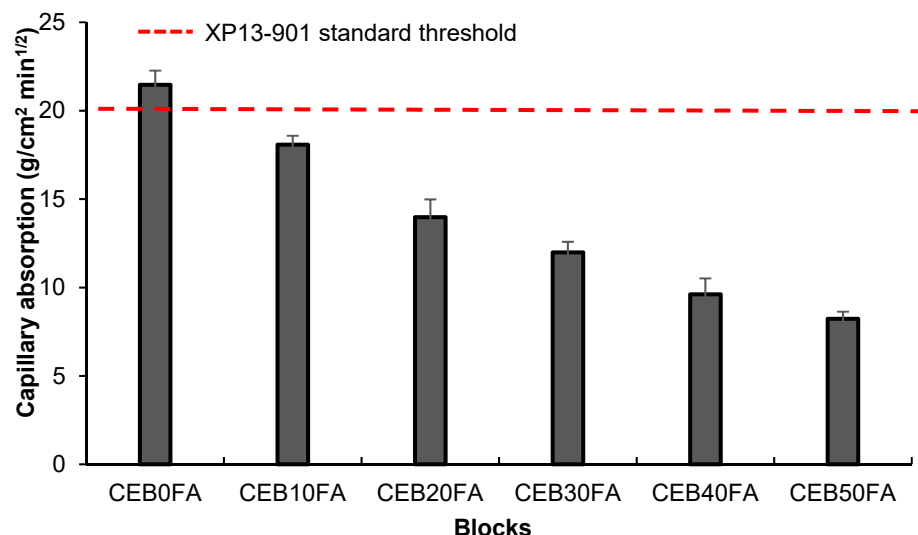


Figure 13. Capillary water absorption coefficient of different CEBs.

Figure 14 shows a linear increase in capillary absorption coefficient with porosity. Therefore, the incorporation of fly ash is expected to improve the water resistance.

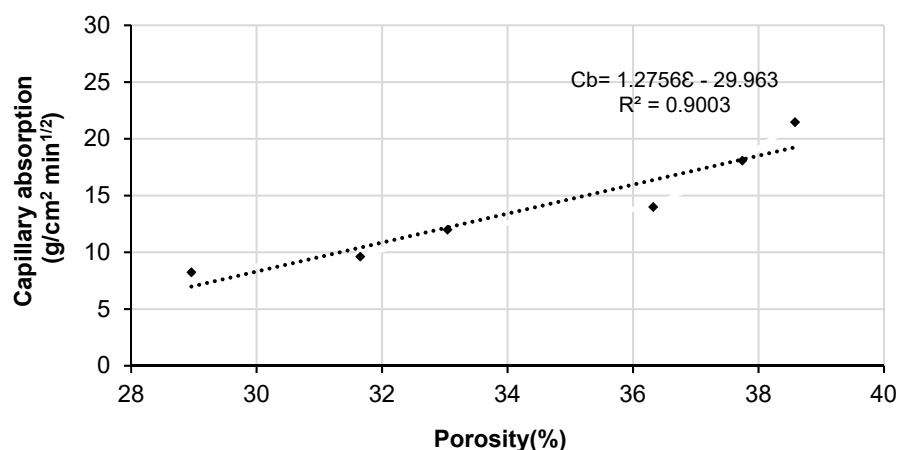


Figure 14. Water absorption by capillary as a function of the porosity of CEBs.

4. Conclusions

The experimental study evaluates the feasibility of using sediment as raw material for the manufacture of compressed earth blocks stabilized by an alkali-activated binder composed of fly ash and sodium hydroxide solution. The physicochemical and thermal characteristics of the CEBs were determined. The following conclusions were obtained:

- The most important factor affecting the mechanical properties was the porosity, since the microstructure of the blocks is modified by the addition of fly ash, as shown in the SEM analysis. The stabilized CEBs showed high mechanical performance which

increased significantly with the fly ash content, although the performance evaluation of these CEBs under unfavorable conditions (wet compressive strength) showed a decrease in compressive strengths of about 50% compared to dry compressive strengths. In addition, all blocks meet the current criteria, which require a minimum compressive strength of 2 MPa.

- The thermal conductivities of the blocks were low, ranging from 0.38 to 0.58 W/m·K. All the blocks fall within the previously documented thermal conductivity range of compressed earth blocks. These CEBs have a good thermal inertia capable to ensure the comfort of the occupants.
- The stabilized blocks with less than 10% fly ash in this study met the criteria indicated in the standards for low-capillary blocks and were perfectly suitable for severe climatic conditions.

Further research concerning the durability performances of CEBs is required. Moreover, these experimental data lead us to suggest that the use of these blocks for bearing masonry structure applications, could provide a solid, durable, and environmentally sustainable construction.

Author Contributions: Conceptualization, M.B. and K.N.; methodology, M.B., K.N. and W.M.; validation, S.A., K.N. and W.M.; formal analysis, M.B., K.N. and W.M.; investigation, M.B., K.N. and W.M.; resources, W.M. and S.A.; data curation, M.B., K.N. and S.A.; writing—original draft preparation, M.B.; writing—review and editing, M.B., K.N., S.A. and W.M.; visualization, K.N., S.A. and W.M.; supervision, K.N., S.A. and W.M.; project administration, S.A. and W.M.; funding acquisition, S.A. and W.M. All authors have read and agreed to the published version of the manuscript.

Funding: This research received no external funding.

Institutional Review Board Statement: Not applicable.

Informed Consent Statement: Not applicable.

Data Availability Statement: The data presented in this study are available on request from the corresponding authors.

Acknowledgments: The study reported in this paper was conducted as part of a partnership agreement between CY Cergy Paris University and IMT Nord Europe. We thank the L2MGC and LGCgE Laboratories.

Conflicts of Interest: The authors declare no conflict of interest.

References

1. Junakova, N.; Junak, J. Sustainable Use of Reservoir Sediment through Partial Application in Building Material. *Sustainability* **2017**, *9*, 852. [\[CrossRef\]](#)
2. Amar, M.; Benzerzour, M.; Safhi, A.E.M.; Abriak, N.-E. Durability of a cementitious matrix based on treated sediments. *Case Stud. Constr. Mater.* **2018**, *8*, 258–276. [\[CrossRef\]](#)
3. Marmin, S.; Dauvin, J.-C.; Lesueur, P. Collaborative approach for the management of harbour-dredged sediment in the Bay of Seine (France). *Ocean. Coast. Manag.* **2014**, *102*, 328–339. [\[CrossRef\]](#)
4. Hadj Sadok, R.; Maherzi, W.; Benzerzour, M.; Lord, R.; Torrance, K.; Zambon, A.; Abriak, N.-E. Mechanical Properties and Microstructure of Low Carbon Binders Manufactured from Calcined Canal Sediments and Ground Granulated Blast Furnace Slag (GGBS). *Sustainability* **2021**, *13*, 9057. [\[CrossRef\]](#)
5. Couvidat, J.; Benzaazoua, M.; Chatain, V.; Bouzahzah, H. Environmental evaluation of dredged sediment submitted to a solidification stabilization process using hydraulic binders. *Environ. Sci. Pollut. Res.* **2016**, *23*, 17142–17157. [\[CrossRef\]](#) [\[PubMed\]](#)
6. Akcil, A.; Erust, C.; Ozdemiroglu, S.; Fonti, V.; Beolchini, F. A review of approaches and techniques used in aquatic contaminated sediments: Metal removal and stabilization by chemical and biotechnological processes. *J. Clean. Prod.* **2015**, *86*, 24–36. [\[CrossRef\]](#)
7. Lirer, S.; Liguori, B.; Capasso, I.; Flora, A.; Caputo, D. Mechanical and chemical properties of composite materials made of dredged sediments in a fly-ash based geopolymer. *J. Environ. Manag.* **2017**, *191*, 1–7. [\[CrossRef\]](#)
8. Bianchi, V.; Masciandaro, G.; Ceccanti, B.; Doni, S.; Iannelli, R. Phytoremediation and Bio-physical Conditioning of Dredged Marine Sediments for Their Re-use in the Environment. *Water Air Soil Pollut.* **2010**, *210*, 187–195. [\[CrossRef\]](#)
9. Caplat, C.; Texier, H.; Barillier, D.; Lelievre, C. Heavy metals mobility in harbour contaminated sediments: The case of Port-en-Bessin. *Mar. Pollut. Bull.* **2005**, *50*, 504–511. [\[CrossRef\]](#)

10. Casado-Martínez, M.C.; Buceta, J.L.; Belzunce, M.J.; DelValls, T.A. Using sediment quality guidelines for dredged material management in commercial ports from Spain. *Environ. Int.* **2006**, *32*, 388–396. [[CrossRef](#)]
11. Dalton, J.L.; Gardner, K.H.; Seager, T.P.; Weimer, M.L.; Spear, J.C.M.; Magee, B.J. Properties of Portland cement made from contaminated sediments. *Resour. Conserv. Recycl.* **2004**, *41*, 227–241. [[CrossRef](#)]
12. Aouad, G.; Laboudigue, A.; Gineys, N.; Abriak, N.E. Dredged sediments used as novel supply of raw material to produce Portland cement clinker. *Cem. Concr. Compos.* **2012**, *34*, 788–793. [[CrossRef](#)]
13. Bouchikhi, A.; Maherzi, W.; Benzerzour, M.; Mamindy-Pajany, Y.; Peys, A.; Abriak, N.-E. Manufacturing of Low-Carbon Binders Using Waste Glass and Dredged Sediments: Formulation and Performance Assessment at Laboratory Scale. *Sustainability* **2021**, *13*, 4960. [[CrossRef](#)]
14. Liu, M. Effects of sintering temperature on the characteristics of lightweight aggregate made from sewage sludge and river sediment. *J. Alloys Compd.* **2018**, *6*, 522–527. [[CrossRef](#)]
15. Xu, Y.; Yan, C.; Xu, B.; Ruan, X.; Wei, Z. The use of urban river sediments as a primary raw material in the production of highly insulating brick. *Ceram. Int.* **2014**, *40*, 8833–8840. [[CrossRef](#)]
16. Hamer, K.; Karius, V. Brick production with dredged harbour sediments. An industrial-scale experiment. *Waste Manag.* **2002**, *22*, 521–530. [[CrossRef](#)]
17. Samara, M.; Lafhaj, Z.; Chapiseau, C. Valorization of stabilized river sediments in fired clay bricks: Factory scale experiment. *J. Hazard. Mater.* **2009**, *163*, 701–710. [[CrossRef](#)]
18. Serbah, B.; Abou-Bekr, N.; Bouchemella, S.; Eid, J.; Taibi, S. Dredged sediments valorisation in compressed earth blocks: Suction and water content effect on their mechanical properties. *Constr. Build. Mater.* **2018**, *158*, 503–515. [[CrossRef](#)]
19. Larbi, S.; Khaldi, A.; Maherzi, W.; Abriak, N.-E. Formulation of Compressed Earth Blocks Stabilized by Glass Waste Activated with NaOH Solution. *Sustainability* **2021**, *14*, 102. [[CrossRef](#)]
20. Achour, R.; Abriak, N.-E.; Zentar, R.; Rivard, P.; Gregoire, P. Valorization of unauthorized sea disposal dredged sediments as a road foundation material. *Environ. Technol.* **2014**, *35*, 1997–2007. [[CrossRef](#)]
21. Serlet, M. Blocs de Terre Comprimée. In *Manuel de Conception et de Construction*; CRAterre: Villefontaine, France, 1995; Volume II, Available online: <https://craterre.hypotheses.org/281> (accessed on 14 November 2021).
22. XP P13-901: Compressed Earth Blocks for Walls and Partitions: Definitions—Specifications—Test Methods—Delivery Acceptance Conditions 2001. Available online: <https://www.boutique.afnor.org/fr-fr/norme/xp-p13901/blocs-de-terre-comprimee-pourmurs-et-cloisons-definitions-specifications-m/fa120503/487> (accessed on 14 November 2021).
23. Houben, H.; Guillaud, H. *Notice “Earth Construction. A Comprehensive Guide”*; Intermediate Technology Development Group Publications: London, UK, 1994; Volume 13.
24. Jiménez Delgado, M.C.; Guerrero, I.C. The selection of soils for unstabilised earth building: A normative review. *Constr. Build. Mater.* **2007**, *21*, 237–251. [[CrossRef](#)]
25. Muntohar, A.S. Engineering characteristics of the compressed-stabilized earth brick. *Constr. Build. Mater.* **2011**, *25*, 4215–4220. [[CrossRef](#)]
26. Yu, H.; Zheng, L.; Yang, J.; Yang, L. Stabilised compressed earth bricks made with coastal solonchak. *Constr. Build. Mater.* **2015**, *77*, 409–418. [[CrossRef](#)]
27. Omar Sore, S.; Messan, A.; Prud’homme, E.; Escadeillas, G.; Tsobnang, F. Stabilization of compressed earth blocks (CEBs) by geopolymer binder based on local materials from Burkina Faso. *Constr. Build. Mater.* **2018**, *165*, 333–345. [[CrossRef](#)]
28. McLellan, B.C.; Williams, R.P.; Lay, J.; van Riessen, A.; Corder, G.D. Costs and carbon emissions for geopolymer pastes in comparison to ordinary portland cement. *J. Clean. Prod.* **2011**, *19*, 1080–1090. [[CrossRef](#)]
29. Rivera, J.; Coelho, J.; Silva, R.; Miranda, T.; Castro, F.; Cristelo, N. Compressed earth blocks stabilized with glass waste and fly ash activated with a recycled alkaline cleaning solution. *J. Clean. Prod.* **2021**, *284*, 124783. [[CrossRef](#)]
30. Davidovits, J. Properties of geopolymer cements. In *First International Conference on Alkaline Cements and Concretes*; Kiev State Technical University Kiev: Kiev, Ukraine, 1994; p. 19. Available online: <https://www.geopolymer.org/wp-content/uploads/KIEV.pdf> (accessed on 14 November 2021).
31. Arrêté du 12 Décembre 2014 Relatif aux Conditions d’Admission des Déchets Inertes dans les Installations Relevant des Rubriques et dans les Installations de Stockage de Déchets Inertes Relevant de la Rubrique 2760 de la Nomenclature des Installations Classées—Légifrance. Available online: <https://www.legifrance.gouv.fr/loda/id/JORFTEXT000029893828/> (accessed on 14 November 2021).
32. EN 450-1; Fly Ash Definition, Specifications and Conformity Criteria. European Committee for Standardization: Brussels, Belgium, 2012.
33. Rifaai, Y.; Yahia, A.; Mostafa, A.; Aggoun, S.; Kadri, E.-H. Rheology of fly ash-based geopolymer: Effect of NaOH concentration. *Constr. Build. Mater.* **2019**, *223*, 583–594. [[CrossRef](#)]
34. Namango, S.S. Development of Cost-Effective Earthen Building Material for Housing Wall Construction: Investigations into the Properties of Compressed Earth Blocks Stabilized with Sisal Vegetable Fibres, Cassava Powder and Cement Compositions. Ph.D. Thesis, Faculty of Environmental Science and Process Engineering of the Brandenburg Technical University Cottbus, Cottbus, Germany, 2006.
35. NF P 94-093. Détermination des références de Compactage d’un Matériau—Proctor Normal et Proctor Modifié. 1999. Available online: <https://pdfslide.net/documents/nf-p-94-093-proctor-99.html> (accessed on 2 September 2021).

36. Preethi, R.K.; Venkatarama Reddy, B.V. Experimental investigations on geopolymer stabilised compressed earth products. *Constr. Build. Mater.* **2020**, *257*, 119563. [[CrossRef](#)]
37. NF-EN 1936. Méthodes d'Essai des Pierres Naturelles—Détermination des Masses Volumiques Réelle et Apparente et des Porosités Ouvertes et Totale. Available online: <https://www.boutique.afnor.org/fr-fr/norme/nf-en-1936/methodes-dessai-pour-pierres-naturelles-determination-des-masses-volumiques/fa041094/49522> (accessed on 13 November 2021).
38. Jaditager, M. Sedimentation and Consolidation Behaviour of Fly Ash-Based Geopolymer Stabilised Dredged Mud. Ph.D. Thesis, James Cook University, Douglas, Australia, 2018. [[CrossRef](#)]
39. Adam, A.A.; Horianto, X.X.X. The Effect of Temperature and Duration of Curing on the Strength of Fly Ash Based Geopolymer Mortar. *Procedia Eng.* **2014**, *95*, 410–414. [[CrossRef](#)]
40. Firdous, R.; Stephan, D.; Djobo, J.N.Y. Natural pozzolan based geopolymers: A review on mechanical, microstructural and durability characteristics. *Constr. Build. Mater.* **2018**, *190*, 1251–1263. [[CrossRef](#)]
41. Touré, P.M.; Sambou, V.; Faye, M.; Thiam, A.; Adj, M.; Azilinson, D. Mechanical and hygrothermal properties of compressed stabilized earth bricks (CSEB). *J. Build. Eng.* **2017**, *13*, 266–271. [[CrossRef](#)]
42. Zhang, Y.M.; Jia, L.T.; Mei, H.; Cui, Q.; Zhang, P.G.; Sun, Z.M. Fabrication, microstructure and properties of bricks fired from lake sediment, cinder and sewage sludge. *Constr. Build. Mater.* **2016**, *121*, 154–160. [[CrossRef](#)]
43. Yoobanpot, N.; Jamsawang, P.; Poorahong, H.; Jongpradist, P.; Likitlersuang, S. Multiscale laboratory investigation of the mechanical and microstructural properties of dredged sediments stabilized with cement and fly ash. *Eng. Geol.* **2020**, *267*, 105491. [[CrossRef](#)]
44. Islam, M.S.; Elahi, T.E.; Shahriar, A.R.; Mumtaz, N. Effectiveness of fly ash and cement for compressed stabilized earth block construction. *Constr. Build. Mater.* **2020**, *255*, 119392. [[CrossRef](#)]
45. Saidi, M.; Cherif, A.S.; Zeghamati, B.; Sediki, E. Stabilization effects on the thermal conductivity and sorption behavior of earth bricks. *Constr. Build. Mater.* **2018**, *167*, 566–577. [[CrossRef](#)]
46. Meukam, P.; Noumowe, A.; Jannot, Y.; Duval, R. Caractérisation thermophysique et mécanique de briques de terre stabilisées en vue de l'isolation thermique de bâtiment. *Mat. Struct.* **2003**, *36*, 453–460. [[CrossRef](#)]
47. Mansour, M.B.; Jelidi, A.; Cherif, A.S.; Jabrallah, S.B. Optimizing thermal and mechanical performance of compressed earth blocks (CEB). *Constr. Build. Mater.* **2016**, *104*, 44–51. [[CrossRef](#)]
48. Gencil, O.; Kazmi, S.M.S.; Munir, M.J.; Sutcu, M.; Erdogmus, E.; Yaras, A. Feasibility of using clay-free bricks manufactured from water treatment sludge, glass, and marble wastes: An exploratory study. *Constr. Build. Mater.* **2021**, *298*, 123843. [[CrossRef](#)]
49. Gueffaf, N.; Rabehi, B.; Boumchedda, K. Recycling Dam Sediments for the Elaboration of Stabilized Blocks. *Int. J. Eng. Res. Afr.* **2020**, *50*, 131–144. [[CrossRef](#)]
50. Réglementation Environnementale RE2020. Available online: <https://www.ecologie.gouv.fr/reglementation-environnementale-re2020> (accessed on 17 November 2021).
51. Réglementation Thermique RT2012. Available online: <https://www.ecologie.gouv.fr/reglementation-thermique-rt2012> (accessed on 17 November 2021).
52. Mimboe, A.G.; Abo, M.T.; Djobo, J.N.Y.; Tome, S.; Kaze, R.C.; Deutou, J.G.N. Lateritic soil based-compressed earth bricks stabilized with phosphate binder. *J. Build. Eng.* **2020**, *31*, 101465. [[CrossRef](#)]